Polymer Journal, Vol. 27, No. 7, pp 673—682 (1995)

Crystallization of Block Copolymers IV. Molecular Weight Dependence of the Morphology Formed in ε-Caprolactone–Butadiene Diblock Copolymers*

Shuichi NOJIMA,*,† Satoru YAMAMOTO,** and Tamaichi ASHIDA**

*School of Materials Science, Japan Advanced Institute of Science and Technology (JAIST), Tatsunokuchi Ishikawa 923-12, Japan
**Department of Biotechnology, School of Engineering, Nagoya University, Nagoya 464-01, Japan

(Received December 8, 1994)

ABSTRACT: The morphology formed in a series of ε-caprolactone–butadiene diblock copolymers (PCL-*b*-PB) has been quantitatively investigated by small-angle X-ray scattering (SAXS) and differential scanning calorimetry(DSC) as a function of total molecular weight ($9400 < M_w < 39400$) of the copolymers with a fixed composition (27 vol% PCL). A sharp X-ray diffraction in the melt was completely replaced with a strong scattering by the crystallization of PCL blocks, suggesting a morphological rearrangement from the microdomain structure into the lamellar morphology (alternating structure consisting of PCL lamellae and amorphous layers). This rearrangement was also confirmed by transmission electron microscopy and polarized microscopy. The spacings of the microdomain structure D and of the lamellar morphology L increased with increasing M_w, though the increasing rates were quite different between D and L. The lamellar thickness, evaluated from a combination of L and bulk crystallinity measured by DSC, was significantly reduced compared with the case of PCL homopolymers, indicating that the lamellar morphology is strongly affected by PB blocks. The scaling analysis of L showed an excellent agreement between the present system and other diblock copolymers with equilibrium morphologies.

KEY WORDS Diblock Copolymer / Microdomain Structure / Crystallization / Small-Angle X-ray Scattering /

The quantitative studies of microdomain structures (lamella, cylinder, or sphere) in amorphous-amorphous diblock copolymers have revealed that the typical size of this structure is intimately dependent on the molecular characteristics of constituent copolymers. The lamellar domain spacing D, for example, changes with molecular weight M as $D \sim M^{2/3}$, as observed for many diblock copolymers.[1-4] The morphology of crystalline homopolymers is well known to be an alternating structure consisting of lamellae and amorphous layers, where characteristic sizes (such as long spacing and lamellar thickness) are not sensitive to M when M is large.[5] In the case of crystalline-amorphous diblock copolymers, we have to consider the equilibrium morphology on the basis of a delicate balance of free energies between deformation of amorphous blocks and chain-folding of crystalline blocks.[6,7] That is, the amorphous block favors a random-coil conformation, resulting in chain-folding of the crystalline block to provide an adequate space for the amorphous block on lamellar surfaces.

There are several theoretical and experi-

* For Part III, see ref 19.
† To whom correspondence should be addressed.

Table I. Characterization of block copolymers used in this study

Notation	Total M_w[a]	M_w/M_n[a]	PCL : PB	Microstructure of PB chain[b]			T_m[c]/°C
			vol %[b]	*cis*-1,4	*trans*-1,4	1,2-Linkage	
B5	9,400	1.05	27 : 73	37	53	10	41
B15	11,300	1.11	27 : 73	35	50	15	43
B11	14,100	1.09	26 : 74	35	51	14	45
B18	26,900 (13,000[d])	1.10	27 : 73	34	53	13	55
B17	39,400	1.38	26 : 74	34	49	17	57
B16	11,400	1.18	47 : 53	37	51	12	51

[a] Values relative to PS standards determined by GPC. [b] Determined by ^{1}H NMR. [c] Determined by DSC. [d] Absolute number-average molecular weight determined by membrane osmometry.

mental studies of the equilibrium morphology of crystalline-amorphous diblock copolymers.[6-16] The experimental studies include a careful evaporation of the solvent to reach the equilibrium state, because the final morphology is determined by an interplay of crystallization and microphase separation. Cohen *et al.*,[13] for example, investigated a path-dependent morphology of a styrene-ethylene diblock copolymer (PS-*b*-PE) and discussed the final morphology on the basis of phase diagram of this PS-*b*-PE + solvent system. Register *et al.*[15] examined the morphology of an ethylene-(ethylene-*alt*-propylene) diblock copolymer, where owing to small interaction between the blocks, crystallization could start from a homogeneous melt without the formation of microdomain structures.

In our previous papers,[17-19] we investigated the crystallization behavior of ε-caprolactone-butadiene diblock copolymers (PCL-*b*-PB) by small-angle X-ray scattering with synchrotron radiation (SR-SAXS), and early and late stages of this phase transition were analyzed by the theories developed for homopolymer crystallizations. This system shows a unique phase transformation because of the intervention of microdomain structures during crystallization. As a result, the late stage of crystallization was significantly affected by the remaining microdomain structure, while the early stage was indistinguishable from that of homopolymer crystallizations.[19] In the present study, we examine the final morphology of PCL-*b*-PB as a function of total molecular weight of the copolymers with a fixed composition. The results are quantitatively compared with other copolymer systems and theoretical predictions. Finally, chain conformations of PCL-*b*-PB in the lamellar morphology are discussed using the numerical results obtained.

EXPERIMENTAL

Materials

The ε-caprolactone-butadiene diblock copolymers (PCL-*b*-PB) with various molecular weights were synthesized by a successive anionic polymerization under vacuum. Details of the synthesis are described elsewhere.[17] The molecular weight relative to polystyrene standards M_w was obtained by gel permeation chromatography (GPC), and the PCL content was evaluated by ^{1}H nuclear magnetic resonance (^{1}H NMR, Varian GEMINI-200)[20] as well as elemental analysis. The results are summarized in Table I.

The following specific volumes were used to calculate the volume fraction of each block in the copolymer. For polybutadiene,[21]

$$v_{sp} = 1.1138 + (8.24 \times 10^{-4})T \qquad (1)$$

and for poly(ε-caprolactone),[22]

$$v_{sp}=0.9106+(6.013\times10^{-4})T \qquad (2)$$

where v_{sp} is in $cm^3\,g^{-1}$ and T is in °C. B5, B15, B11, B18, and B17 have a constant composition (*ca.* 27 vol% PCL) with various molecular weights ($9400<M_w<39400$), and the PB blocks in various copolymers all have the similar microstructure (*cis*-1,4, *trans*-1,4, or 1,2-linkage), so that interaction between the PCL and PB blocks is expected to be the same. B16 was prepared to check the morphology before and after crystallization by transmission electron microscopy (TEM), because a meaningful picture could not be obtained with the PB-rich copolymers due to difficulty in getting a thin section.

The absolute molecular weight M_n' of B18 was also measured by membrane osmometry to quantitatively compare the molecular weight dependence of the morphology with that of other systems. M_n' of the others was estimated from the ratio of M_n' and M_n (obtained from GPC) assuming that the ratio relating absolute and PS-equivalent molecular weights is independent of M_n for the copolymers with a fixed composition.

B5 and B15 are homogeneous in the melt from the fact that the SAXS curve shows a diffuse scattering due to the *correlation hole effect* of block copolymers.[23,24] B11, B18, and B17 are, on the other hand, microphase separated into mosaic structures composed of lamellae and cylinders, which are deduced from the angular positions of SAXS intensity peaks. B16 has a lamellar microdomain structure in the melt, as observed by TEM (Figure 1a).

Small-Angle X-ray Scattering (SAXS) Measurements

Two SAXS techniques were used according to the structural spacing in the samples; conventional SAXS (C-SAXS) for shorter spacing samples (up to 20 nm) and synchrotron SAXS (SR-SAXS) for longer spacing samples.

The C-SAXS measurement was performed with a pinhole collimation system and a one-dimensional position sensitive proportional counter (PSPC).[25] The time necessary for each measurement was 3000 s, during which the sample was kept at crystallization temperature T_c within the fluctuation of 0.1°C. The SR-SAXS measurement was carried out at National Laboratory for High Energy Physics, Tsukuba, Japan (Photon Factory), with Small-Angle X-ray Equipment for Solution (SAXES) installed on a Beamline BL-10C. Details of the optics and the instrumentation are described elsewhere.[17,26] The SAXS intensity was accumulated during a period of 300 s.

The SAXS intensity measured was corrected for the decrease in the ring current (for SR-SAXS), background scattering, and finally Lorentz factor. Since the optics of both C-SAXS and SR-SAXS is *point* focusing, the scattered intensity was not corrected for the smearing effect by the finite cross section of the primary beam.[26]

Microscopic Observations

The morphology of B16 before and after crystallization was observed by transmission electron microscopy (TEM). The sample was first stained with O_sO_4 at *ca.* 70°C ($>T_m$) and room temperature ($<T_m$) for 24 hours to fix the microdomain structure and lamellar morphology, respectively. The sample was then cooled to room temperature and subsequently sectioned by ultramicrotomy to observe the fixed morphology at each temperature.

The spherulitic superstructure was observed by polarized microscopy with a hot stage.[27] The temperature of this stage was controlled by circulating water of a constant temperature, and crystallization was started by dropping the water temperature from *ca.* 65°C to a crystallization temperature T_c. The sample thickness prepared was about 0.02 mm.

Differential Scanning Calorimetry (DSC) Measurements

A MAC Science Model 3100 DSC was used to determine the melting temperature and

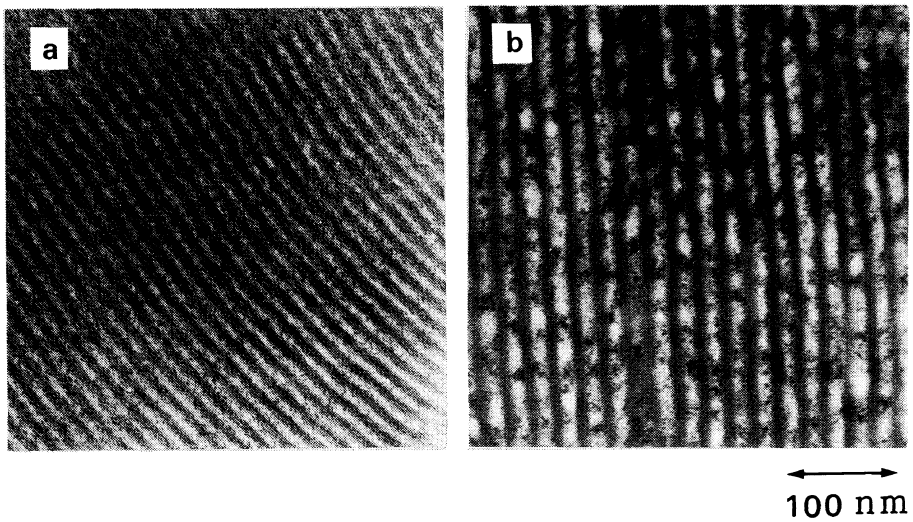

Figure 1. Transmission electron micrographs of (a) the lamellar microdomain structure for B16 at 70°C ($> T_m$) and (b) the lamellar morphology for B16 at 25°C ($< T_m$). The dark portion is the PB block stained by O_sO_4.

crystallinity of PCL blocks. The sample, first annealed at *ca.* 60°C for 1—2 h, was quenched into T_c and then heated at a rate of 5°C min^{-1}. The quench process was performed in the DSC cell, and it took about 1 min for the sample to be completely quenched to T_c during which PCL blocks did not start to crystallize. The crystallinity and melting temperature of PCL blocks were evaluated from the peak area and peak position of the endothermic curve. The exothermic heat flow during crystallization was also monitored to ensure the end of crystallization at each T_c.

RESULTS

Microscopic Observations

In our recent SR-SAXS studies,[17-19] we qualitatively observed the behavior of morphological rearrangement by the crystallization of PCL blocks; a diffraction arising from the microdomain structure was steadily replaced with a strong scattering from the lamellar morphology. Figure 1, observed by TEM for B16 before and after crystallization, clearly visualizes this rearrangement. Figure 1a shows the lamellar microdomain structure in the melt with a domain spacing $D \sim 13$ nm and Figure 1b the lamellar morphology (alternating structure of PCL lamellae and amorphous layers) with a long spacing $L \sim 20$ nm. These values of D and L correspond consistently to those obtained by SAXS measurements described below. Figure 1 confirms that the microdomain structure is completely destroyed by the subsequent crystallization of PCL blocks, and the lamellar morphology certainly spreads over the system.

The typical superstructures after crystallization at 25°C observed by polarized microscopy are shown in Figure 2 for B11 (26 vol% PCL) (a) and B16 (47 vol% PCL) (b). There is a remarkable difference in spherulitic superstructures; B11 shows less-developed spherulites with polarized fragments localized at each center of the spherulite. The similar superstructures were observed for all other copolymers with the same composition, and also similar in appearance with that observed by Lovinger *et al.*[16] on a PCL-poly(dimethyl siloxane)-PCL copolymer (40% PCL). The spherulite observed for B16 is, on the other

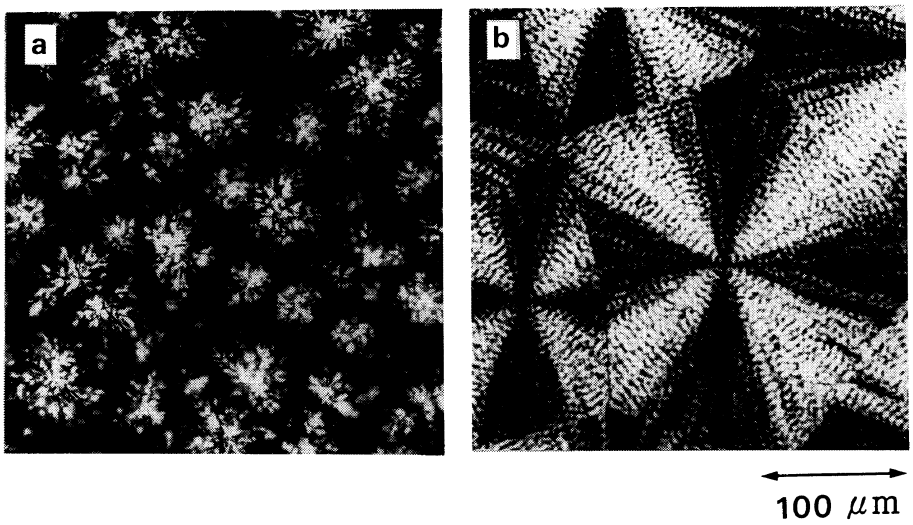

Figure 2. Polarized micrographs of (a) B11 crystallized at 25°C and (b) B16 at 25°C.

hand, well-developed, though the inside is open in texture compared with that of PCL homopolymer.[27,28] In addition, the spherulite has regular extinction rings, which are characteristic of the binary blend of PCL and PB.[27] Figure 2 indicates that the crystallization of PCL blocks yields spherulitic superstructures as well as lamellar morphologies, that is, the lamellar crystals formed in PCL-*b*-PB are systematically organized to result in spherulitic superstructures as in the case of homopolymer crystallizations. This fact also confirms the structural rearrangement by crystallization over the microdomain structure in the melt.

SAXS Measurements

The dramatic change of morphologies shown in Figure 1 is also expected to appear in SAXS curves. Figure 3 shows the X-ray intensity curves scattered from B16 at various temperatures indicated. At temperatures above T_m, a sharp diffraction corresponding to $D=15.3$ nm is observed, which is almost independent of temperature. This diffraction arises from the microdomain structure in the melt (Figure 1a). In SAXS curves below T_m, on the other hand, a strong intensity maximum appears at a lower angle, which arises from the lamellar morphology (Figure 1b). Every SAXS curve below T_m has a diffuse hump (indicated by arrows) at the position corresponding to strictly twice the angular position of the first intensity maximum. The angular position of these intensity humps indicates the well-ordered *lamellar* morphology, as shown in Figure 1b. The lamellar morphology is experimentally observed for several systems, such as ethylene oxide-*t*-butyl methacrylate diblock copolymer (PEO-*b*-PTBMA)[14] and ethylene-(ethylene-*alt*-propylene) diblock copolymer (PE-*b*-PEP),[15] with relatively small compositions (down to 10%) of crystallizable block.

The peak position shifts slightly toward a lower angle with increasing T_c, resulting in the increase of L with T_c. For example, L is 21.7 nm at $T_c=31.1$°C and 24.1 nm at $T_c=40.2$°C. The variation of L with T_c can be more or less observed for all çopolymers studied. The increase of L with T_c is usually observed for the crystallization of homopolymers; the lamellar thickness l_c increases and the amorphous layer thickness l_a decreases with increasing T_c to yield the increase of bulk crystallinity. In the present case, however, the bulk

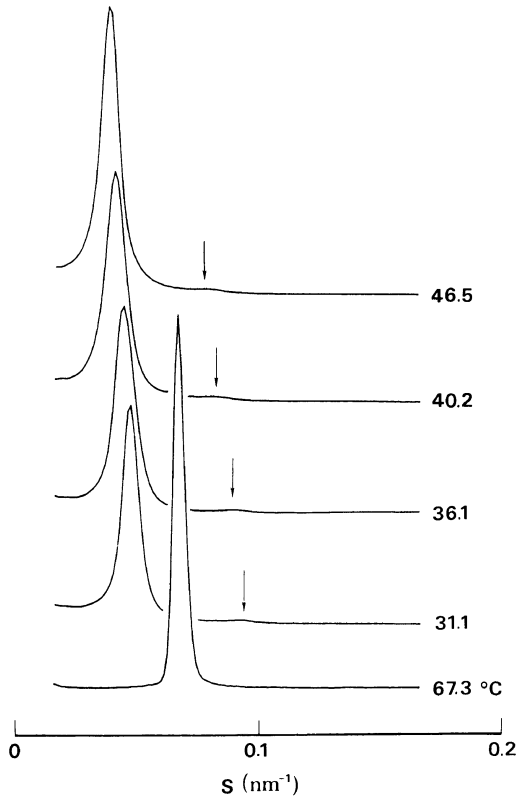

Figure 3. X-ray intensities, scattered from B16 at each temperature indicated, are plotted against s ($=2\sin\theta/\lambda$). The SAXS curve at 67.3°C, enlarged by a factor of 5 for clarity, arises from the microdomain structure of the copolymer (Figure 1a), and all the others from the lamellar morphology (Figure 1b).

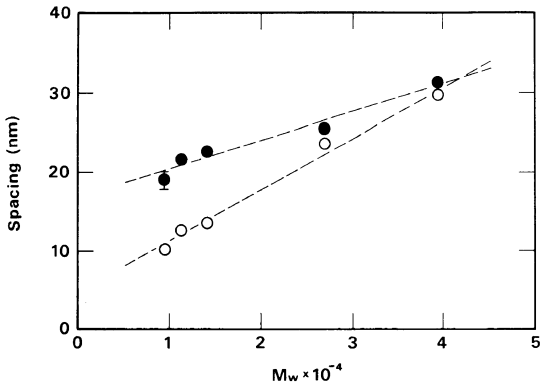

Figure 4. Spacings, evaluated from the angular position of the X-ray intensity maximum scattered from microdomain structure (○) and lamellar morphology (●), are plotted against M_w. The error bar represents the variation range of L with T_c.

crystallinity does not change significantly with T_c, suggesting that the lamellar morphology does not change with increasing T_c. In addition, the morphology (*i.e.*, l_c, l_a, and crystallinity) is also comparable to that in the copolymer slowly cast from toluene (good for both blocks), which is expected to have the morphology close to the equilibrium state. These facts suggest that the morphology formed by quenching from the melt is very close to the equilibrium state. Two factors, low molecular weight of the copolymers (Table I) and low T_g of the constituent blocks (below −80°C for PB[29] and *ca.* −60°C for PCL[30]), will be important for attaining the equilibrium morphology. Since the variation of L with T_c is small compared to that with M_w, it does not affect the following results at all (Figure 4).

The M_w dependence of the domain spacing D (of microdomain structure) and the long spacing L (of lamellar morphology) is shown in Figure 4 where the variation of L mentioned above is denoted by an error bar. The values of D and L increase significantly with M_w, though the two slopes are quite different, reflecting the difference in the mechanism of morphology formation between microphase separation and crystallization.

DSC Measurements

Typical DSC thermograms are depicted in Figure 5 for the copolymers crystallized at 25°C. The melting endothermic curves for B5 and B11 are diffuse with the melting temperature T_m lower than B17 and B18, while those for B17 and B18 are similar in shape to that of PCL homopolymers, suggesting that the PCL block length significantly affects the lamellar thickness and therefore melting behavior in this molecular weight range; for B5, B15, and B11, PCL blocks are not long enough to make thick lamellae as observed in homopolymers, so that T_m and crystallinity reduce as a result of thin

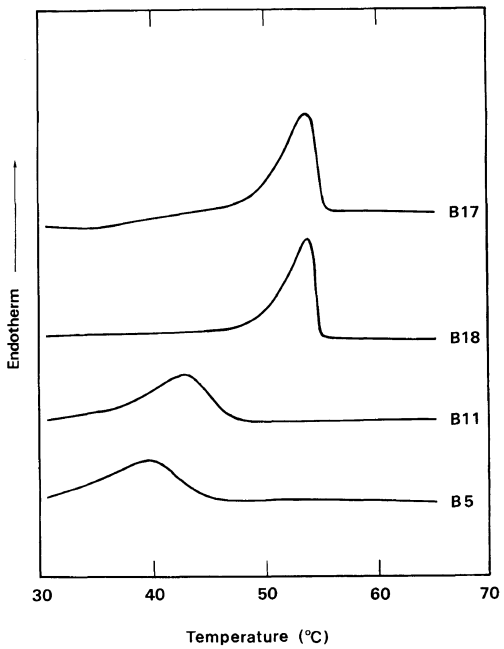

Figure 5. DSC thermograms for the copolymers crystallized at 25°C. The heating rate is 5°C min^{-1}.

and immature lamellae. Since PCL blocks of B17 and B18 are sufficiently long, their lamellae are similar to those formed in PCL homopolymers to give the usual thermal behavior.

Figure 6 shows the M_w dependence of PCL block crystallinity χ evaluated as,

$$\chi = \Delta H/(\Delta H^\circ f) \tag{3}$$

where ΔH is the heat of fusion per gram of copolymers, ΔH° that of perfect PCL crystal (135.44 J g^{-1})[22], and f the weight fraction of PCL blocks. In the figure, the error limit of χ was also depicted, which increases in magnitude with decreasing M_w. The change of χ with M_w is reminiscent of the molecular weight dependence of characteristic values in synthetic polymers such as T_g and T_m; in the oligomeric range they increase with M_w and finally level off at high M_w. Since B5, B15, and B11 do not have enough PCL block length to crystallize in the same manner with polymers, details of the morphology (such as chain-folding and chain-packing) may change significantly with

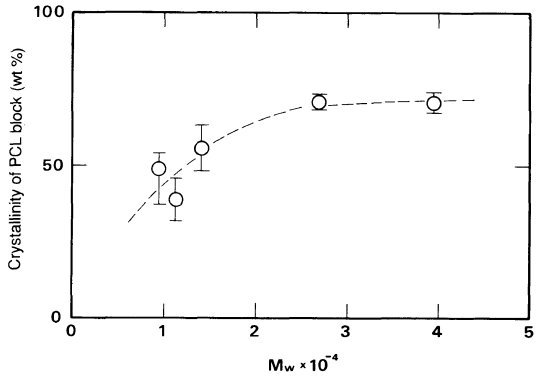

Figure 6. PCL block crystallinity χ evaluated from DSC thermogram is plotted against M_w.

M_w and are sensitive to the crystallization condition to yield a large error in estimating χ, as shown in Figure 6.

If we assume that the lamellar morphology, an alternating structure of PCL lamellae and amorphous layers as observed in Figure 1b, prevails in the system, then it is possible to calculate l_c and l_a from a combination of L and χ.[31] Figure 7 shows the M_w dependence of l_c and l_a, where both l_c and l_a increase with M_w, though l_a is much larger than l_c. The large value of l_a suggests the insertion of PB blocks between PCL lamellae. The unexpected small value of l_c for lower molecular weight samples ($\sim$2.5 nm) is probably ascribed to short PCL blocks, and consequently leads to the low T_m shown in Figure 6. The chain conformation of PCL and PB blocks in the lamellar morphology is discussed later.

DISCUSSION

Comparison with Theories and Other Experimental Results

The molecular weight dependence of equilibrium morphologies for crystalline-amorphous diblock copolymers is theoretically predicted by DiMarzio *et al.*[6] and Whitmore and Noolandi,[7] where the morphology is assumed to be an alternating structure consisting of lamellae and amorphous layers. The repeating

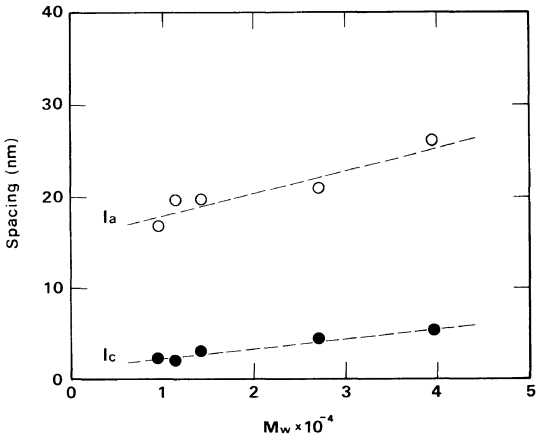

Figure 7. Lamellar thickness (●) and amorphous layer thickness (○) evaluated from Figures 4 and 6 are plotted against M_w.

distance of this structure L, which corresponds to the long spacing evaluated from SAXS measurements, is expected in a scaling form as:

$$L \propto Z_t Z_a^{\beta} \tag{4}$$

where Z_t and Z_a represent the segment number of the whole copolymer and of the amorphous block, respectively. The value of β is either $-1/3$ (DiMarzio *et al.*) or $-5/12$ (Whitmore and Noolandi). Therefore, the plot of $\log(L/Z_t)$ *vs.* $\log Z_a$ should give a straight line with the slope of β, as discussed by Cohen *et al.*[11] and Register *et al.*[15]

Figure 8 shows such a plot of the present data, together with other experimental results made with an ethylene-(ethylene-*alt*-propylene) diblock copolymer (PE-*b*-PEP) by Register *et al.*[15] and an ε-caprolactone-(dimethyl siloxane)-ε-caprolactone triblock copolymer (PCL-*b*-PDMS) by Lovinger *et al.*[16] For evaluating Z_t and Z_a, segment molecular weight was assumed to be $60\,g\,mol^{-1}$ for PCL and PB blocks to get the consistency among the data for different systems.[15] Figure 8 shows that our data agree well with those for PE-*b*-PEP and PCL-*b*-PDMS, and all make a straight line over a wide range of $\log Z_a$. The excellent agreement in magnitude of L/Z_t between our results and the data for other systems, where microdomain structures never appear, indicates that the present copolymers can attain the equilibrium morphology even from the microdomain structure in the melt. Figure 8 also suggests that the scaling relation represented by eq 4 holds qualitatively for the equilibrium morphology of crystalline-amorphous block copolymers.

The slope of the line including all data in Figure 8 is $-0.54\,(\pm 0.04)$, slightly smaller than the predicted values ($-1/3$ or $-5/12$). Donth *et al.*[14] obtained $\beta = -0.53$ for the equilibrium morphology of ethylene oxide-*t*-butyl methacrylate diblock copolymer (PEO-*b*-PTBMA). By considering the experimental uncertainties, they concluded the conformity with the theoretical predictions. In the present case, one possibility to yield such discrepancy in β might be the estimation of Z_t and Z_a. We used a same segment molecular weight ($=60\,g\,mol^{-1}$) for estimating Z_t and Z_a as a first approximation. The use of statistical segment length appropriate to each block to evaluate Z_t and Z_a might yield a significant change in β.

Chain Conformation in Lamellar Morphology

The SAXS and TEM results suggest that the morphology after crystallization is an alternating structure consisting of lamellae and amorphous layers (lamellar morphology) even for PCL-*b*-PB with 27 vol% PCL. This fact is also supported by the morphological studies of other crystalline-amorphous diblock copolymers with small compositions of crystallizable block. Here, we consider the chain conformation of B18 in the lamellar morphology, because the absolute molecular weight of B18 is directly evaluated by membrane osmometry (Table I).

The X-ray structural analysis shows that the conformation of PCL homopolymer in the crystal is almost planar zigzag with fiber period (*c* axis) of 1.705 nm in which two monomers are contained.[32] The lamellar thickness l_c of

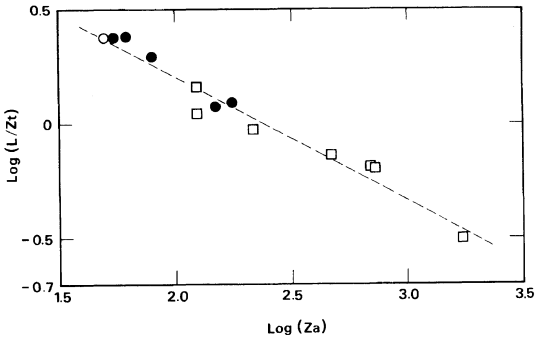

Figure 8. The scaling plot with various experimental data. Z_t and Z_a represent the segment number of the whole copolymer and of the amorphous block, respectively. □, data by Register *et al.*,[15]; ○, data by Lovinger *et al.*,[16]; ●, present results.

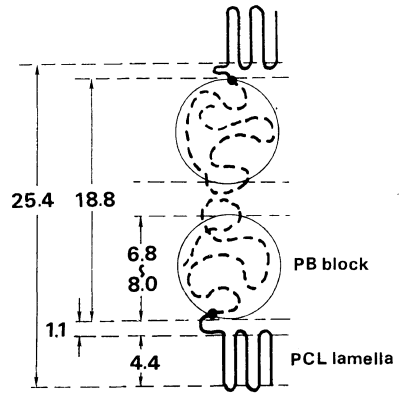

Figure 9. Schematic illustration of chain conformation of B18 in the lamellar morphology. The numerals in the figure are in nm.

B18 crystallized at 25°C is 4.4 nm, so that the number of monomers consisting of a stem, m, is about 5 if we assume that the PCL stem is perpendicular to the lamellar surface. The number of folds n_f of PCL blocks is then calculated as

$$n_f = \frac{\left(\frac{M}{M_0}\right) f}{m} - 1 \qquad (5)$$

where M is molecular weight of PCL blocks ($=4000\,g\,mol^{-1}$), M_0 monomer molecular weight ($=114\,g\,mol^{-1}$), and f crystallinity of PCL blocks ($=0.71$ by weight). We finally obtain $n_f=4$ for B18.

The amorphous layer thickness l_a is evaluated to be 21.0 nm, which is composed of PB blocks and uncrystallized PCL blocks. If we assume that PB and PCL blocks segregate completely within the amorphous layer without any interface layer (see Figure 9), the layer thickness of PB blocks l'_a is 18.7 nm from a volume ratio between PB and PCL blocks. Since PB blocks emanate from both sides of the amorphous layer, one PB block has to occupy the space with the thickness of $l'_a/2=$ 9.35 nm. The diameter of PB blocks d ($=2\langle S^2\rangle^{1/2}$) with M in the unperturbed state can be calculated from the end to end distance of PB homopolymers,[33] as

$$d/2=\langle S^2\rangle^{1/2}=\frac{a}{\sqrt{6}}M^{1/2} \qquad (6)$$

where a is in the range between 0.082 and 0.103 nm depending on the microstructure (*cis*, *trans*, or 1,2-linkage) of PB blocks. The absolute molecular weight of PB blocks is 9000, so that d is estimated to be 6.4—8.0 nm. Above numerical calculations show that $l'_a/2$ is slightly larger than the diameter of PB blocks in the unperturbed state.

The chain conformation of B18 including both PCL and PB blocks is schematically illustrated in Figure 9, which is plausible from the viewpoint of theoretical predictions.[6,7] That is, the amorphous PB block is slightly enlarged and also the number of folds of PCL blocks increases. These significant changes in the conformation of both blocks will give a favorable morphology for crystalline-amorphous diblock copolymers.

Acknowledgments. We would like to thank Dr. Hironari Sano of Mitsubishi Chemicals Co. for the help of TEM observations. This work was supported in part by Grants-in-Aid for Scientific Research (No 06651046) from the Ministry of Education, Science, and Culture of Japan, and has been performed under the approval of the Photon Factory Program

Advisory Committee (Proposal No. 93G088).

REFERENCES

1. D. J. Meier, "Block and Graft Copolymers;" J. J. Burke and V. Weiss, Ed., Syracuse University Press, Syracuse, N.Y., 1973.
2. E. Helfand, *Macromolecules*, **8**, 552 (1975).
3. T. Hashimoto, M. Shibayama, and H. Kawai, *Macromolecules*, **13**, 1237 (1980).
4. Y. Matsushita, K. Mori, R. Saguchi, Y. Nakao, I. Noda, and M. Nagasawa, *Macromolecules*, **23**, 4313 (1990).
5. B. Wunderlich, "Macromolecular Physics," Vol. 1, Academic Press, New York, N.Y., 1973.
6. E. A. DiMarzio, C. M. Guttman, and J. D. Hoffman, *Macromolecules*, **13**, 1194 (1980).
7. M. D. Whitmore and J. Noolandi, *Macromolecules*, **21**, 1482 (1988).
8. T. Vilgis and A. Halperin, *Macromolecules*, **24**, 2090 (1991).
9. I. S. Zemel, J. P. Corrigan, and A. E. Woodward, *J. Polym. Sci.*, **B27**, 2479 (1989).
10. R. Seguela and J. Prud'homme, *Polymer*, **30**, 1446 (1989).
11. K. C. Douzinas, R. E. Cohen, and A. F. Halasa, *Macromolecules*, **24**, 4457 (1991).
12. C. V. Veith, R. E. Cohen, and A. S. Argon, *Polymer*, **32**, 1545 (1991).
13. R. E. Cohen, P. L. Cheng, K. Douzinas, P. Kofinas, and C. V. Berney, *Macromolecules*, **23**, 324 (1990).
14. R. Unger, D. Beyer, and E. Donth, *Polymer*, **32**, 3305 (1991).
15. P. Rangarajan, R. A. Register, and L. J. Fetters, *Macromolecules*, **26**, 4640 (1993).
16. A. J. Lovinger, B. J. Han, F. J. Padden, Jr., and P. A. Mirau, *J. Polym. Sci.*, **B31**, 115 (1993).
17. S. Nojima, K. Kato, S. Yamamoto, and T. Ashida, *Macromolecules*, **25**, 2237 (1992).
18. S. Nojima, H. Nakano, and T. Ashida, *Polym. Commun.*, **34**, 4168 (1993).
19. S. Nojima, H. Nakano, Y. Takahashi, and T. Ashida, *Polymer*, **35**, 3479 (1994).
20. E. R. Santee, Jr., R. Chang, and M. Morton, *J. Polym. Sci., Polym. Lett. Ed.*, **11**, 449 (1973).
21. D. Rigby and R. J. Roe, *Macromolecules*, **19**, 721 (1986).
22. V. Crescenzi, G. Manzini, G. Calzolari, and C. Borri, *Eur. Polym. J.*, **8**, 449 (1972).
23. K. Mori, H. Hasegawa, and T. Hashimoto, *Polym. J.*, **17**, 799 (1985).
24. S. Nojima and R. J. Roe, *Macromolecules*, **20**, 1866 (1987).
25. S. Nojima, M. Ono, and T. Ashida, *Polym. J.*, **24**, 1271 (1992).
26. S. Nojima, K. Kato, M. Ono, and T. Ashida, *Macromolecules*, **25**, 1922 (1992).
27. S. Nojima, D. Wang, and T. Ashida, *Polym. J.*, **23**, 1473 (1991).
28. S. Nojima, K. Watanabe, Z. Zheng, and T. Ashida, *Polym. J.*, **20**, 823 (1988).
29. F. S. Dainton, D. M. Evans, F. E. Hoare, and T. P. Melia, *Polymer*, **3**, 297 (1962).
30. J. V. Koleske and R. D. Lundberg, *J. Polym. Sci., Polym. Phys. Ed.*, **7**, 795 (1969).
31. F. B. Khambatta, F. Warner, T. Russell, and R. S. Stein, *J. Polym. Sci., Polym. Phys. Ed.*, **14**, 1391 (1976).
32. Y. Chatani, Y. Okita, H. Tadokoro, and Y. Yamashita, *Polym. J.*, **1**, 555 (1970).
33. J. Brandrup and E. H. Immergut, Ed., "Polymer Handbook," 3rd ed, Wiley-Interscience, New York, N.Y., 1989, VII-33.